Chemistry & Biology, Vol. 9, 925–931, August, 2002, ©2002 Elsevier Science Ltd. All rights reserved. PII S1074-5521(02)00188-6

Targeting DNA Bulged Microenvironments with Synthetic Agents: Lessons from a Natural Product

Zhen Xi,[1,5] Geum-Sook Hwang,[1] Irving H. Goldberg,[1,4] Jeffrey L. Harris,[2] William T. Pennington,[2] Farid S. Fouad,[3,5] Ghassan Qabaja,[3] Justin M. Wright,[3] and Graham B. Jones[3,4]

[1]Department of Biological Chemistry and Molecular Pharmacology
Harvard Medical School
Boston, Massachusetts 02215
[2]Molecular Structure Center
Department of Chemistry
Clemson University
Clemson, South Carolina 29634
[3]Bioorganic & Medicinal Chemistry Laboratories
Department of Chemistry
Northeastern University
Boston, Massachusetts 02115

Summary

Bulged regions of nucleic acids are important structural motifs whose function has been linked to a number of key nuclear processes. Additionally, bulged intermediates have been implicated in the etiology of several genetic diseases and as targets for viral regulation. Despite these obvious ramifications, few molecules are capable of selective binding to bulged sequences. Prompted by the remarkable affinity of a natural product metabolite, we have designed and prepared a series of readily accessible synthetic agents with selective bulge binding activity. Furthermore, by screening a library of bulge-containing oligodeoxynucelotides, correlations between structure and affinity of the agents can be drawn. In addition to potential applications in molecular biology, the availability of these spirocyclic agents now opens the door for rational drug design.

Introduction

Nucleic acids can have richly diverse structures, including hairpins, knots, pseudoknots, triple helices, loops, helical junctions, and bulges (Figure 1) [1]. Such bulged structures in nucleic acids are of general biological significance [2]. They have been proposed as intermediates in a multitude of processes including RNA splicing, frame-shift mutagenesis, intercalator-induced mutagenesis, imperfect homologous recombination, as the binding site for the coat protein of bacteriophage, and in the ribosomal synthesizing machinery [3]. Bulges have also been suggested as binding motifs for regulatory proteins involved with viral replication, including the TAR region of HIV-1 [4-6]. Additionally, the etiology of at least 12 human neurodegenerative genetic diseases has been attributed to genetic variations in the lengths of triplet repeats in genomic DNA (e.g., myotonic dystrophy, Huntington's disease, Friederich's ataxia, and fragile X syndrome). The unstable expansion of triplet repeats has been attributed to reiterative synthesis due to slippage and *bulge formation in the newly formed DNA strand* [7-10]. As such, compounds capable of binding to bulges could have significant therapeutic potential. Despite these obvious ramifications, few previous attempts have been made to prepare compounds with affinity for bulged sequences. Success has been hindered by lack of an available substrate that can effectively mimic the base pairing involved at a bulged site, which requires a unique wedge-shaped template.

The most promising bulge-specific agent discovered to date originated from work on the enediyne natural product NCS-chrom [11]. This antitumor antibiotic typically undergoes cellular thiol addition and subsequent cycloaromatization to produce arene **2** (Figure 2), a process that goes through a diyl radical intermediate, which induces DNA strand scission, accounting for the biological activity of the agent. However, in the absence of thiols, NCS-chrom undergoes an alternate general base catalyzed intramolecular cyclization to generate a spirocyclic radical [12] that specifically cleaves bulged structures (2–3 unpaired bases) in DNA and RNA [13-15]. In the absence of bulged DNA, NCS-chrom undergoes spontaneous cyclization to form the spirocyclic arene **3** [16], an isostructural mimic of the DNA-cleaving species. Though having minimal affinity for duplex DNA, **3** binds specifically to a synthetic bulged DNA mimic at submicromolar concentration [17], and solution phase NMR studies have confirmed that the binding to the bulge emanates from the unique molecular geometry of the agent [18, 19]. A solution structure of the complex reveals that the wedge-shaped molecule fits tightly in the triangular prism pocket formed by the two looped-out bases and the neighboring base pairs. In the bulge pocket, the two ring systems of **3** mimic the geometry of the helical bases with a twist angle of $\sim 35^\circ$ and stack with the base pairs above and below. Further, **3** is able to induce bulge formation in otherwise unstructured regions of DNA [19]. The capacity for **3** to recognize bulges stems specifically from the orientation of the ring systems, transposed approximately 60° by the spirolactone, and the right-handed 35° twist of the molecule [18, 19]. Given the ramifications of such selective binding, this has prompted effort to explore the specificity of bulge bindings and, ultimately, design and synthesize readily accessible bulge selective compounds.

Results and Discussion

In order to survey the selectivity afforded by **3**, we first synthesized a variety of bulge- and hairpin-containing oligodeoxyribonucleotides and associated control elements, and their putative fold patterns are shown in Figure 3. Binding of **3** to these substrates was monitored using fluorescence spectroscopy and provided striking

[4]Correspondence: irving_goldberg@hms.harvard.edu (IHG), gr.jones@neu.edu (GBJ)
[5]These authors contributed equally to this work.

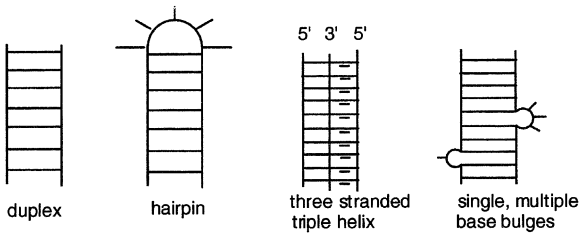

Figure 1. Assorted Nucleic Acid Conformations

results (Table 1). As expected, affinity of **3** for a 12-mer duplex sequence was low (entry 1), whereas affinity for a GT bulge containing counterpart was pronounced (entry 2). Since the thermal stability of short duplexes is lower than that of their hairpin counterparts (Tm: entry 1, 44°; entry 2, 32°; entry 3, 65°; entry 14, 80°), we also assessed affinity for various hairpin-constrained analogs containing **1**, 2, and 3 base bulges (entries 3–6). Clearly, affinity for the 2 base bulge is optimal (entry 4), and a panel of GT bulge containing 12-mers with different backbone sequences were then screened (entries 7–12). As can be seen, striking differences in affinity result from subtle modification in sequence, confirming the high order of molecular recognition that **3** imparts [17]. In particular, replacement of the T•A base pair 3′ to the bulge site with an A•T base pair leads to marked loss in binding affinity (and in cleavage at the bulge [14]). Finally, the residual contribution of the hairpin sequences was assessed with additional controls (entries 13–15), confirming that the hairpin itself is a somewhat more accessible target than the corresponding duplex (cf. entries 1, 14).

The nanomolar affinity in many cases (entries 3, 4, 10, and 16) is remarkable, as is the preference for 2 base bulges [14, 17, 18], and bodes well for drug development. Since the results were so promising, we set about design of readily available mimics of **3** that might evolve into potential drug candidates. Based on analysis of the binding data for **3**, NMR, and molecular modeling studies (PM3), it is clear that the key features responsible for 2 base-bulge binding are (i) the presence of two independent aromatic π systems, (ii) a spirocyclic ring junction capable of offsetting the systems by 30°–40°, and (iii) a pendant aminosugar moiety to enhance binding to the phosphate backbone at the bulged site (Figure 4). One option would be to produce modified analogs of **3**. However, though several excellent approaches to NCS-chrom and analogs have been reported [20-23], the complexity of the syntheses effectively preclude use of the natural product as a template, requiring scratch synthesis. Further, we sought a more stable structure than the lactone ring system. Based on these design criteria, we instead reasoned that aldol product **4** (Figure 5), presumably available via ketoaldehyde **5**, would be an acceptable and readily available *synthetic* template from which to build and install the aminosugar moiety, having a predicted helical twist very similar to **3** and providing the option for introduction of variable functional groups [24].

Accordingly, a synthesis was devised and executed (Figure 6). Diels-Alder cycloaddition of the cyclopentenone derived from in situ elimination of **6** with the diene **7** (derived from tetralone) gave cycloadduct **8**. Oxidative cleavage to give **9** followed by aldol closure gave hydroxyketone **10** in good yield, isolated as a mixture of enantiomers and accompanied by 25% of its exo isomer. The design criteria now called for addition of an aminosugar moiety. Though compound **10** could be separated into its enantiomer pairs via chiral chromatography, we elected to perform diastereomer separation following glycosylation. An aminoglucose was selected as the pendant aminosugar group for reasons of simplicity and economy. Thus, β-aminoglucose was converted to activated derivative **11**, subjected to acidic coupling with racemic **10** to give a mixture of diastereomers, which were separable by silica gel chromatography, and then subjected to global deprotection to give enantiomers **12** and **13**. Though unfortunately not amenable to X-ray analysis, structures **12** and **13** were fully assignable by COSY and CD-ORD spectroscopy (see SI) [25].

The derivatives were then screened alongside **3** for affinity to the battery of bulged and duplex sequences. It became immediately apparent that the simple derivatives were able to mimic the natural product-derived agent **3** effectively (Table 1). Enantiomers **12/13** had very similar affinity to that of **3** for the 2 base bulge sequence (entry 2), and affinity for the duplex (entry 1) and unmodified hairpin (entry 13) was low. Of significance, differential affinity between **12** and **13** for selected *bulged* sequences emerged, highlighting the bias that the stereochemistry imparts (entries 3, 4, 5, and 7). Though **3** overall had gross affinity vastly higher to specific bulged targets (entries 3, 4, 10, and 16), in several cases the synthetic agents showed improved affinity to **3** (entries 5, 7, 8, and 9). Of note, variations within the bulged family are evident, which provide crucial information as to the architecture of the bulged target. Agent **3** shows poorer affinity than **12/13** for the single bulged sequence (entry 5), presumably due to the steric bulk of the additional functionality present. Likewise, a switch from pyrimidine to purine base 3′ to the bulge results in marked reduction in affinity for **3** (entries 7, 8 versus 3), whereas

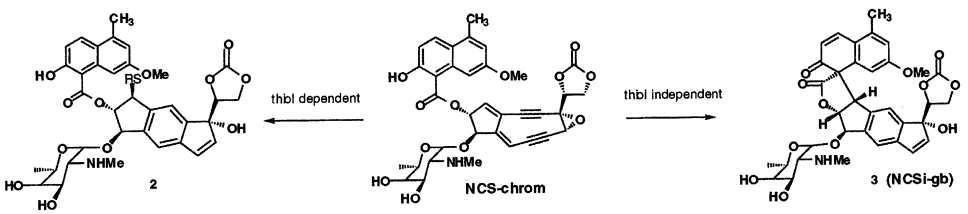

Figure 2. Activation Cascade of Neocarzinostatin Chromophore in Presence or Absence of Thiol

Entry	Sequence Code	Conformation	Entry	Sequence Code	Conformation
1	DA12:DAc12	5'-GTCCGATGCGTG 3'-CAGGCTACGCAC	9	HT3GGTA	5'-GTCCGTCGCGTG T 3'-CAGGCAGCGCAC T TG
2	DA12:BA14	5'-GTCCGATGCGTG 3'-CAGGCTACGCAC TG	10	HT3GGTT	5'-GTCCGACGCGTG T 3'-CAGGCTGCGCAC T TG
3	HT3AGTT	5'-GTCCGATGCGTG T 3'-CAGGCTACGCAC T TG	11	HT3GGTC	5'-GTCCGGCGCGTG T 3'-CAGGCCGCGCAC T TG
4	HT4AGTT	5'-GTCCGATGCGTG T T 3'-CAGGCTACGCAC T TG	12	HT3CGTC	5'-GTCCGGGGCGTG T 3'-CAGGCCCCGCAC T TG
5	HT3AGT	5'-GTCCGATGCGTG T 3'-CAGGCTACGCAC T G	13	HT3TA	5'-GTCCGTAGCGTG T 3'-CAGGCATCGCAC T
6	HT3AGCTT	5'-GTCCGATGCGTG T 3'-CAGGCTACGCAC T TG C	14	HT3AT	5'-GTCCGATGCGTG T 3'-CAGGCTACGCAC T
7	HT3AGTA	5'-GTCCGTTGCGTG T 3'-CAGGCAACGCAC T TG	15	HT3AA	5'-GTCCGTTGCGTG T 3'-CAGGCAACGCAC T
8	HT3TGTA	5'-GTCCGTAGCGTGT 3'-CAGGCATCGCAC T TG T	16	PEG4ATT	5'-CCCGATGC 3'-GGGCTACG TA

Figure 3. Synthetic Oligonucleotides

the relative effect on the synthetic agents was less pronounced, implying subtle differences in binding orientation (cf. **12/13** entry 7). This observation is consistent with an earlier proposal, based on NMR studies [18,19], that removal of the bulky cyclic carbonate moiety of **3** would obviate the discriminating effect of the sequence change on drug binding. Since efforts to interpret these differences would be greatly assisted by X-ray data for the template, we pursued and were able to solve the structure for **10** (Figure 7A). As can be seen, by virtue of the spirocyclic junction, the two aromatic frameworks are clearly offset, presenting a helical twist (~35°) and establishing a wedge with a cone angle of ~32°. Superimposition of the three-dimensional structures of **3** and **10** reveals their striking similarities (Figures 7B and 7C). This finding is of particular interest, since the structure of **3** is NMR derived from its form in the complex with bulged DNA and reflects binding pocket-induced conformational changes in which the two drug ring systems are brought closer together [19], whereas the structure of **10** is that found in the crystal, presumably reflecting crystal-induced compaction. A similar change may be expected to occur in the synthetic drug-bulged DNA

Table 1. Dissociation Constants (μM) of DNA Binding (Figure 3) by the Drugs*

Entry	Sequence Code	3	12	13
1	DA12:DAc12	307	31.1	32.8
2	DA12:BA14	2.18	5.33	2.54
3	HT3AGTT	0.033	1.34	0.46
4	HT4AGTT	0.026	1.21	0.53
5	HT3AGT	20.6	9.71	1.75
6	HT3AGCTT	0.71	5.74	3.04
7	HT3AGTA	12.5	11.0	2.67
8	HT3TGTA	22.2	3.16	3.26
9	HT3GGTA	12.9	6.0	5.0
10	HT3GGTT	0.064	1.59	1.03
11	HT3GGTC	0.416	2.53	2.74
12	HT3CGTC	0.50	1.46	1.48
13	HT3TA	16.9	16.9	17.6
14	HT3AT	10	14.0	7.6
15	HT3AA	13.7	20.7	17.5
16	PEG4ATT	0.081	4.05	1.52

*Determined via emission spectra [λ_{exc} 390 nm (**3**), 310 nm (**12/13**); λ_{emm} 400–600 nm (**3**), 350–550 nm (**12/13**)] using a slit width 2.0, and a scan speed of 100 nm/min at 5°C.

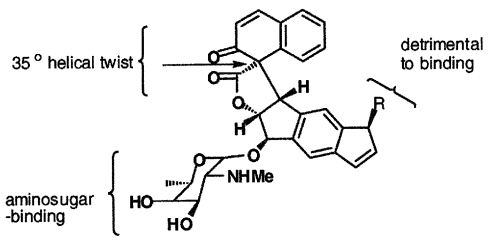

Figure 4. Structure-Affinity Correlation for NCSi-gb

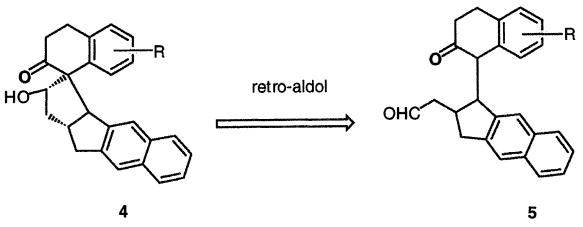

Figure 5. Structure of 4 + 5

complex. The NMR-derived model of the ethylene glycol linked bulged sequence (Table 1, entry 16) [18,19] clearly suggests that the prism-shaped binding pocket of the bulge would be accessible to the template of **10**, and that further nonbonded interactions with the DNA would be expected from the aminosugar moiety (Figure 4). The high affinity binding of **3** and the synthetic agents to this sequence confirms this affinity (entry 16), and now provides us with a topological model from which to design analogs. Further, it is expected that placement of the aminosugar on the oxygen moiety of the 6-membered ring bicyclic system, akin to the naphthoate of the natural product, will enhance bulge selectivity. Indeed, given the potential for a combinatorial library approach to synthesis, it is reasonable to expect that rationally designed systems, including those with reactive functionalities capable of alkylation or strand cleavage, can now be designed to address specific bulged targets of interest.

Significance

Our work confirms that simple readily accessible synthetic agents can show selectivity as bulge binders. The prerequisite for binding is the presence of a fused spirocyclic motif coupled to a pendant aminosugar moiety. The availability of these agents has allowed us to probe factors governing affinity to bulged sequences and the stability of the bulged motif as a function of oligonucleotide structure. Our results indicate that spirocyclic agents prefer a 2 base bulged target on an oligodeoxynucelotide that contains a 3 base hairpin. Armed with these data, functional assays can now be designed to allow us to explore the dynamics of bulge formation and the ramifications of bulge binding in cellular events. With this work, the unsolved problem of small molecule binding to an important class of nucleic acid conformation has finally been addressed.

Experimental Procedures

Preparation of Base Postactivated NCS-Chrom (NCSi-gb, 3)
NCS-chrom was isolated from the holoantibiotic NCS with 0.5 M acetic acid in methanol and stored at –80°C as described [16]. General-base postactivated NCS chrom (NCSi-gb) was prepared by incubation of NCS-chrom (100 μM) in 50 mM Tris-HCl (pH 8.5), 50% ethanol in the absence of DNA at 0°C for 1 hr. Following lyophilization of the reaction mixture, the dried sample was redissolved in 100 mM ammonium acetate at pH 4.0 and subjected to HPLC purification on a reverse-phase C-18 column. Purification and isolation of **3** was accomplished by using a linear gradient of 40%–65% solvent B/solvent A over a 40 min period (solvent A, aqueous 5 mM ammonium acetae [pH 4.0]; solvent B, methanolic 5 mM ammonium acetate [pH 4.0]; flow rate, 1 ml/min).

6,8,8a,9,15b,15c-Hexahydro-5H-Benzo[5,6]Indeno-[2,1-c]Phenanthren-9-One(8)
To a 250 ml round-bottom flask equipped with a reflux condenser was added 3-bromobenz[*f*]indan-1-one (4.0 g, 15.38 mmol) [26], 2-vinyl-3,4-dihydronapthalene (**7**) (3.27 g, 20.91 mmol) [27], and carbon tetrachloride (65 mL). The resulting solution was heated to reflux and Et_3N (1.95 g, 19.23 mmol) in carbon tetrachloride (40 mL) was added dropwise. The solution was refluxed for 3.0 hr and then poured onto water (100 mL). The layers were separated and the

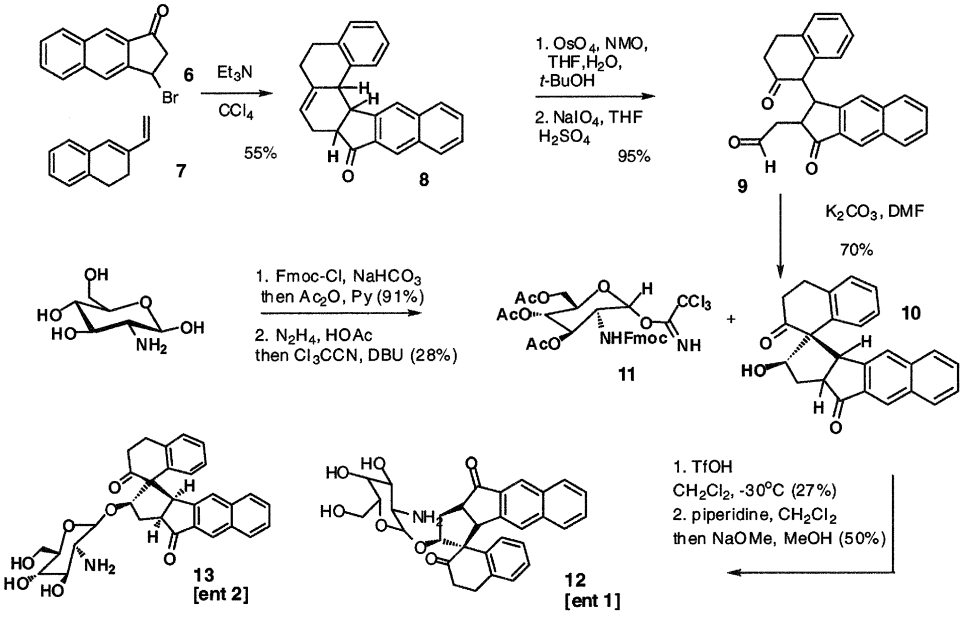

Figure 6. Intramolecular Aldol-Glycosylation Sequence for NCSi-gb Mimics

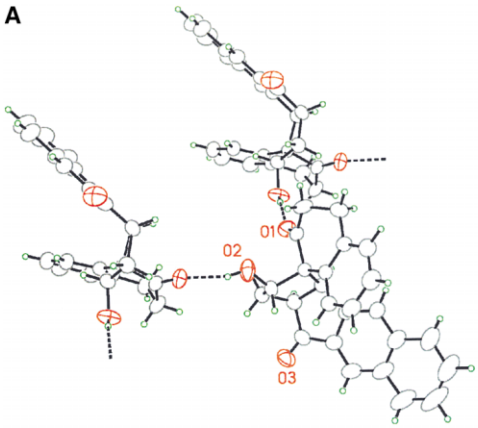

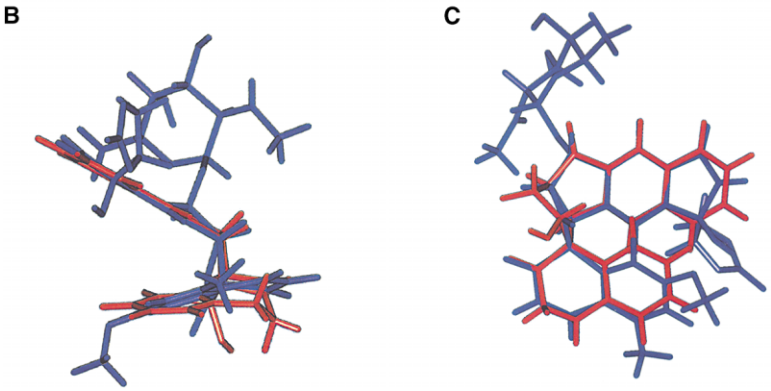

Figure 7. Structures of Synthetic and Natural Products

(A) ORTEP of spiroalcohol **10** showing hydrogen bonding.

(B and C) Overlapped structures of NCSi-gb (blue) and synthesized spiroalcohol (red), respectively.

NCSi-gb structure is from NMR structure of NCSi-gb-bulge-DNA complex [18] and spiroalcohol structure is from X-ray crystallographic structure. Side view (A) and top view (B) show similarity of twist angle (~35°) and rise (~3Å) of the two ring systems of the two structures.

aqueous layer was extracted with Et_2O (3 × 100 mL). The combined organic extracts were washed with 1% HCl (3 × 200 mL), saturated $NaHCO_3$ solution (2 × 200 mL), brine (3 × 200 mL), dried over $MgSO_4$, and concentrated in vacuo. The crude oil was purified by gradient silica gel chromatography (0:100 to 3:100, Et_2O:hexanes) to yield the title compound (2.85 g, 55%) as a yellow solid, mp 148°C–149°C; ^1H NMR δ 8.18 (s, 1H), 7.89 (m, 2H), 7.58 (d, 1H, *J* = 7.44 Hz,), 7.44 (m, 3H), 7.34 (m, 2H), 7.02 (d, 1H, *J* = 7.71 Hz), 5.68 (m, 1H), 4.16 (t, 1H, *J* = 7.44 Hz), 3.96 (d, 1H, *J* = 6.45 Hz), 3.17 (ddd, 1H, *J* = 8.19, 8.19, 1.95 Hz), 2.98 (m, 1H), 2.35 (m, 1H), 2.22 (m, 1H) 2.10 (m, 2H), 1.20 (m, 1H); ^{13}C NMR δ 210.1, 147.5, 141.0, 139.8, 137.1, 136.5, 136.1, 132.1, 130.0, 129.0, 128.2, 128.08, 128.0, 126.9, 126.4, 126.1, 125.9, 122.8, 120.5, 48.8, 45.9, 42.3, 30.3, 29.1, 25.3; $C_{25}H_{20}$,O requires: C, 89.25; H, 5.99; found: C, 89.32; H, 6.01.

2-[1-Oxo-3-(2-Oxo-1,2,3,4-Tetrahydro-1-Naphthalenyl)-2,3-Dihydro-1H-Cyclopenta[b]Naphthalen-2-yl] Acetaldehyde(9)

Osmium tetroxide (5% aqueous solution, 1 mL) was added to a mixture of **9** (1.35g, 4.018 mmol), 4-methylmorpholine N-oxide (0.68g, 5.02 mmol), THF (40 mL), acetone (8 mL), *t*-BuOH (5 mL), and water (15 mL). The resulting mixture was stirred at room temperature for 13 hr, then sodium dithionate (2 g) was added and stirring continued for 15 min. The mixture was diluted with EtOAc (200 mL), washed with water (2 × 50 mL), and brine (50 mL), dried (Na_2SO_4) and condensed in vacuo. The resulting white residue was dissolved in THF (150 mL), then sodium periodate (2.2g, 10.28 mmol), and H_2SO_4 (1.0 N, 1 mL) was added; the resulting heterogeneous mixture was stirred for 4 hr. The mixture was diluted with ether (150 mL), washed with water (2 × 100 mL), dried (Na_2SO_4), and condensed in vacuo to produce a residual solid, which was recrystallized from chloroform/hexanes to give the title compound (1.40g, 95%) as a white solid mp 160°C–162°C; ^1H NMR ($CDCl_3$) δ 10.13 (s, 1H), 8.29 (s, 1H), 7.95 (d, 1H, J = 7.0 Hz), 7.56 (t, 2H, J = 8.0 Hz), 7.42–7.52 (m, 3H), 7.37 (t, 1H, J = 7.5 Hz), 7.21 (d, 1H, J = 7.5 Hz), 6.9 (s, 1H), 4.44 (dd, 1H, J = 8.5 and 2.4 Hz), 3.76 (m, 2H), 3.45 (m, 1H), 3.21 (dd, 1H, J = 20 and 9.9 Hz), 2.6–2.72 (m, 1H), 2.2–2.4 (m, 1H), 1.9–2.04 (m, 2H). ^{13}C NMR δ 210.45, 203.99, 202.20, 145.00, 137.42, 136.58, 134.75, 132.95, 130.51, 129.82, 128.54, 128.23, 128.09, 127.85, 127.56, 126.71, 124.26, 124.10, 50.78, 48.50, 48.32, 42.69, 40.63, 28.16; $C_{25}H_{20}O_3$ requires: C, 81.50; H, 5.47. Found: C, 81.70; H, 5.35.

Spirocyclic Alcohol (10)

Ketaldehyde (**9**) (1.2 g, 3.26 mmol) was dissolved in DMF (150 mL) the solution cooled to 0°C for 10 min, then potassium carbonate (1.35g, 9.78 mmol) was added, and the resulting mixture stirred at 0°C for 10 min. The mixture was diluted with ether (150 mL), washed with water (2 × 100 mL) and brine (100 mL), dried (Na_2SO_4), and condensed in vacuo. Purification by SGC (100% ether) gave spiroalcohol **10** (0.85g, 70%) as a white solid mp 163°C–164°C; ^1H NMR ($CDCl_3$, 300 MHz): δ 8.28 (s, 1H), 7.93 (m, 1H), 7.42–7.52 (m, 2H), 7.1–7.4 (m, 2H), 7.2–7.3 (m, 1H), 6.87 (t, 1H, J = 8.1 Hz), 6.55 (d, 1H, J = 8.1 Hz), 6.42 (s, 1H), 4.41 (d, 1H, J = 1H, J = 11.4 and 7.5 Hz), 3.58 (ddd, 1H, J = 16.5, 11.7, and 6.0 Hz), 3.36 (ddd, 1H, J = 12.3, 9.0, and 0.9 Hz), 3.32 (ddd, 1H, J = 15.9, 6.9, and 2.1), 3.2 (ddd, 1H, J = 16.0, 7.0, and 2.1 Hz), 3.06 (ddd, 1H, J = 17.1, 5.7, and 2.7 Hz), 2.7–2.9 (m, 2H), 2.6 (ddd, 1H, J = 12.3, 7.2, and 1.5 Hz). ^{13}C NMR δ 213.95, 208.5, 145.04, 138.60, 136.87, 135.4, 135.0, 132.60, 130.31, 128.82, 128.71, 128.32, 128.20, 127.90, 127.1, 127.0, 126.90, 124.50, 75.30, 64.60, 48.0, 46.50, 38.60, 35.10, 29.00; $C_{25}H_{20}O_3$ requires: C, 81.50; H, 5.47. found: C, 81.45; H, 5.51. Also isolated, exo isomer (0.29 g, 24%); ^1H NMR ($CDCl_3$, 300 MHz): δ 8.27 (d, 1H, J = 6 Hz), 7.95 (t, 1H, *J* = 7.2 Hz), 7.71 (d, 1H, *J* = 7.8 Hz), 7.56 (d, 1H, *J* = 7.2 Hz), 7.52–7.42 (m, 3H), 7.37 (d, 1H, *J* = 7.2 Hz), 7.33–7.26 (m, 2H), 4.86 (dd, 1H, *J* = 10 and 7.5 Hz), 4.32 (d, 1H, *J* = 9.5 Hz), 3.33

(m, 1H), 2.84–2.68 (m, 3H), 2.45 (m, 2H), 2.15 (m, 1H); ^{13}C NMR δ 211.8, 207.3, 145.0, 138.5, 138.5, 136.6, 136.3, 133.1, 130.7, 128.9, 128.5, 127.9, 127.8, 127.4, 126.7, 126.5, 124.3, 123.1, 87.4, 64.2, 54.9, 48.3, 42.3, 43.1, 28.2; HRMS: calculated for $C_{25}H_{20}O_3$ 368.1412; found 368.1411.

1,3,4,6- Tetra-O-Acetyl-2-Deoxy-2-(9-Fluorenylmethoxycarbonylamino)-D-Glucopyranose

D-glucosamine hydrochloride (9.0 g, 41.77 mmol) and $NaHCO_3$ (10 g, 118.5 mmol) were dissolved in water (120 mL), and cooled to 0°C. A solution of 9-fluorenylmethyl chloroformate (6 g, 23.2 mmol) in dioxane (60 mL) was added, and the mixture stirred for 1 hr. at room temperature. The resulting white precipitate was filtered and washed with water (3 × 25 mL), dried via anisotropy (toluene, 2 × 40 mL), and then dissolved in dry pyridine (80 mL). Acetic anhydride (80 mL) was added and the mixture was stirred for 12 hr at 25°C, poured onto water/crushed ice (250 mL), and stirred vigorously to give a white precipitate. The precipitate was filtered and the residue washed with water (3 × 50 mL), 2% HCl (3 × 50 mL), saturated $NaHCO_3$ (1 × 50 mL), and water (1 × 50 mL), and then dried via anisotropy (toluene, 2 × 50 mL) to yield of the title compound (12 g, 91%) as a white powder; ^{1}H NMR ($CDCl_3$, 300 MHz): δ 7.75 (d, 2H, *J* = 7.5), 7.53 (t, 2H, *J* = 8), 7.39 (t, 2H, *J* = 7.5), 7.30 (d, 2H, *J* = 7), 6.2 (d, J = 3.3, α H-1), 5.74 (d, J = 8 Hz, β-H1), 5.3–4.9 (m, 2H), 4.45–4.95 (m, 7H), 2.20 (s, 1H), 2,09, 206, 2.04, 2.00 (4s,12H), ^{13}C NMR δ 171.2,170.9, 169.6, 168.9, 155.9, 155.8, 143.8, 143.75, 141.5, 128.0, 127.3, 125.2, 120.3, 92.7, 91.0, 73.0, 72.5, 70.7, 69.9, 68.1, 67.8, 67.4, 61.9, 61.8, 55.2, 47.2, 47.15, 21.2, 20.95, 20.8; HRMS: calculated. for C_{29} H_{31} N O_{11} 569.1897; found 569.1895.

3,4,6-Tri-O-Acetyl-2-Deoxy-2-(9-Fluorenylmethoxycarbonylamino)-β-D-Glucopyranosyltrichloroacetimidate(11)

A solution of 1,3,4,6-tetra-O-acetyl-2-doexy-2-(9-fluorenylmethoxycarbonylamino)-D-glucopyranose (12 g, 21.1 mmol) in dry DMF (100 mL) was treated with hydrazinium acetate (2 g, 21.7 mmol) and stirred for 50 min at 25°C. It was then diluted with ethyl acetate (600 mL), washed with brine (4 × 200 mL), and dried ($MgSO_4$). Volatiles were removed in vacuo and the remaining oil was azeotroped with dry benzene (2 × 50 mL). The residual oil was dissolved in dry CH_2Cl_2 (100 mL) then trichloroacetonitrile (15 mL, 103.9 mmol) and DBU (1.8 mL, 12 mmol) were added, and the mixture stirred at 25°C for 45 min. The solution was condensed in vacuo, then the residual oil was purified by SGC (1:1 ethyl acetate/hexanes) to yield the title compound (4.0 g 28%) as a pale yellow powder; ^{1}H NMR ($CDCl_3$, 500 MHz): δ 8.80 (d,1H, *J*= 3.5 Hz), 7.75 (d, 2H, *J* = 8 Hz), 7.51 (d, 2H, *J* = 7 Hz), 7.39 (t, 2H, *J* = 7 Hz), 7.29 (t, 2H, *J* = 8 Hz), 6.38 (d,1H, *J* = 4 Hz), 5.45 (dd, 1H, *J* = 9.5, 3), 5.35 (t,1H, *J* = 10), 5.27 (t, 1H, *J* = 9.5), 5.02 (d, 1H, *J* = 9.5), 4.55 (ddd, 1H, *J* = 11, 7.5, 2), 4.42–4.10 (m, 5H), 2.09, 2.06, 2.05 (3s,9H),^{13}C NMR δ 170.5, 169.1, 169.0, 160.2, 155.4, 150.7, 143.3, 141.1, 127.6, 126.9, 124.8, 119.9, 94.7, 70.2, 70.1, 67.3, 61.3, 60.3, 53.4, 46.8, 20.6; HRMS: calculated for C_{29} H_{29} Cl_3 N_2 O_{10} 670.0888; found 670.0891.

Aminoglucose Coupling Reaction

A suspension of spiroalcohol **10** (0.1 g, 0.27 mmol), trichloroacetimidate **11** (0.340 g, 0.51 mmol), and 3 Å molecular sieves (0.20 g) in CH_2Cl_2 (4.0 mL) was prepared in a 10 ml round-bottom flask and the mixture was cooled to –30°C under Ar. Triflic acid (0.1 mL, 0.33 M in CH_2Cl_2) was added dropwise over 2 min. The resulting solution was warmed to 25°C over 3 hr, then diluted to 50 ml with CH_2Cl_2, filtered, and the filtrate washed with a saturated solution of sodium bicarbonate (2 × 15 mL). The organic phase was dried ($MgSO_4$) concentrated in vacuo, and the crude product purified by radial chromatography (silica gel, 1 mm, 30% ethyl acetate/hexanes) to give the coupling products corresponding to the *3,4,6-tri-O-acetyl-2-deoxy-2-(9-fluorenylmethoxycarbonylamino)-β-D-glucopyranosyl* derivatives of **10** as individual diastereomers: diastereomer A, isolated (40 mg, 17%) as a white solid (R_f 0.33 silica gel, 1:1 ethyl acetate/ hexanes); ^{1}H NMR ($CDCl_3$, 500 MHz): δ 8.3 (s, 1H), 7.95 (s, 1H), 7.775 (d, 2H, *J* = 7.5 Hz), 7.62 (d, 2H, *J* = 7.5 Hz), 7.57 (t, 2H, *J* = 8 Hz), 7.47 (m, 1H), 7.40 (t,2H, *J* = 7.5 Hz), 7.35 (dd, 1H, *J* = 7.5, 3 Hz), 7.31 (t, 2H, *J* = 7.5 Hz), 7.20 (m, 1H), 7.04 (t, 1H, *J* = 7.5 Hz), 6.48 (bs, 1H), 6.40 (s,1H), 5.87 (d, 1H, *J* = 8 Hz), 5.33 (t, 2H, *J* = 10 Hz), 5.828 (s, 2H), 5.21 (d, 2H, *J* = 10 Hz), 5.13 (t, 2H, *J* = 10 Hz), 4.43 (m, 1H), 4.31 (m, 1H), 4.21 (m, 2H), 4.13 (m,2H), 4.04 (dt, 1H, *J* = 10.5, 3.5 Hz), 3.65 (bs, 1H), 3.41(m, 1H), 3.20 (m, 1H), 3.07 (m, 1H), 2.73 (m, 1H), 2.59 (m, 1H), 2.05 (s, 3H), 2.04 (s, 3H), 1.95 (s, 3H); ^{13}C NHR δ 211.6, 209.1, 171.0, 170.7, 169.6, 155.9, 146.5, 143.9, 141.5, 138.3, 136.9, 135.2, 132.6, 130.4, 129.2, 128.8, 128.3, 127.9, 127.5, 127.4, 127.3, 126.9, 126.8, 125.3, 124.3, 120.2, 103.0, 91.7, 71.1, 68.5, 67.9, 63.8, 62.2, 56.1, 50.7, 50.3, 47.3, 41.6, 33.0,31.1, 29.4, 20.8; HRMS: calculated for C_{52} H_{47} N O_{12} 877.3098; found 877.3099.

Diastereomer B, isolated (23 mg, 10%) as a white solid (R_f 0.2 - silica gel, 1:1 ethyl acetate/ hexanes); ^{1}H NMR ($CDCl_3$, 500 MHz): δ 8.31 (s, 1H), 7.97 (s, 1H), 7.77 (d, 2H, *J* = 7.5 Hz), 7.47 (d, 2H, *J* = 9.0 Hz), 7.41 (m, 5H), 7.30 (m,4H), 6.95 (bs, 1H), 6.77 (m, 1H), 6.37 (s,1H), 5.8 (d, 1H, *J* = 8 Hz), 5.06 (s, 1H), 4.93 (s, 1H), 4.48 (d, 2H, *J* = 6.5 Hz), 4.32 (t, 2H, *J* = 3 Hz), 4.28-4.22 (m, 2H), 4.15 (m, 1H), 4.07 (m, 1H), 3.99–3.93(m, 3H), 3.52 (t, 2H, *J* = 10.5 Hz), 3.13 (m, 1H), 2.96 (m, 1H), 2.78–2.65 (m, 2H), 2.05 (s, 3H), 1.99 (s, 6H), ^{13}C NMR δ 209.3, 207.3, 171.1, 170.9, 169.6, 155.2, 146.4, 143.9, 141.5, 138.5, 136.8, 135.9, 132.6, 130.3, 128.9, 128.7, 128.6, 128.2, 128.1, 127.9, 127.2, 126.7, 126.8, 125.4,.125.3, 125.2, 124.1, 120.2, 102.5, 89.4, 71.9, 68.8, 66.9, 63.8, 62.4, 56.1, 51.3, 49.7, 47.0, 41.6, 33.3, 31.1, 29.6, 21.0, 20.8; HRMS: calculated for (M + H): 877.3176; found 878.3176

Spirocylic Aminoglucose Conjugates (12 & 13)

The individual, fully protected aminogluco-pyranosyl spiro compound diastereomer A (20 mg, 0.028 mmol) was dissolved in a solution of piperdine (10% in CH_2Cl_2, 0.5 mL) and stirred for 45 min at 25°C. Volatiles were removed and the residue was dissolved in anhydrous methanol (3 mL) and cooled to 0°C. A solution of NaOMe in methanol (0.5 ml of 1.0 M) was added and the reaction warmed to 25°C and stirred for an additional 1 hr. The reaction was quenched with water (0.5 mL), volatiles were removed, and then the crude residue purified via gradient radial chromatography (1.0 mm, 1:1 ethyl acetate/hexanes to 100% ethyl acetate) to yield **12** (6 mg, 50%) as a colorless oil. Similar treatment of diastereomer B gave **13** (48%) as a colorless oil.

(12): ^{1}H NMR(500MHz, CD_3OD) δ 8.28 (s, 1H), 7.99 (m, 1H), 7.48 (m, 2H), 7.39 (m, 1H), 7.34 (d, J = 7.5Hz, 1H), 7.12 (t, J = 7.5 Hz, 1H), 6.58 (t, J = 7.6 Hz, 1H), 6.50 (s, 1H), 6.16 (d, J = 7.6 Hz, 1H), 4,62 (dd, J = 10.5, 7.4 Hz, 1H), 4.35 (d, J = 8.0 Hz, 1H), 4.00 (d, J = 7.9 Hz, 1H), 3.78 (dd, J = 12.3, 2.4 Hz, 1H), 3.62 (dd, J = 12.5, 5.5 Hz, 1H), 3.46(dd, J = 12.9, 8.6 Hz, 1H), 3.35 (ddd, J = 12.5, 3.6 Hz, 1H), 3.20 (m, 2H), 3.02 (dd, J = 10.5, 9.0, 1H), 2.96 (m, 1H), 2.83 (m, 2H), 2.81 (ddd, J = 15.5, 11.0, 1.6 Hz, 1H), 2.58 (ddd, J = 13.0, 7.5, 2.4Hz, 1H), 2.45 (dd, J = 12.3, 8.1 Hz, 1H) ; ^{13}C NMR (125.6 MHz, CD_3OD) δ 214.5, 211.0, 147.4, 139.6, 137.7, 137.0, 135.8, 133.4, 130.7, 129.6, 129.3, 128.9, 128.7 127.7, 127.2, 126.2, 124.4, 103.4, 86.0, 77.3, 76.4 70.8, 64.2, 61.8, 57.6, 51.3, 50.1, 41.3, 33.6, 29.0; HRMS: calculated for C_{31} H_{31} N O_7 529.2100; found 529.2105

(13): ^{1}H NMR(500 MHz, CD_3OD) δ 8.23 (s, 1H), 7.95 (m, 1H), 7.46 (m, 2H), 7.35 (m, 1H), 7.28 (d, J = 7.5 Hz, 1H), 7.04 (t, J = 7.5 Hz, 1H), 6.53 (t, J = 7.5 Hz, 1H), 6.48 (s, 1H), 6.16 (d, J = 7.5 Hz, 1H), 4,67 (dd, J = 10.0, 7.7 Hz, 1H), 4.40 (d, J = 8.0 Hz, 1H), 4.22 (d, J = 7.8 Hz, 1H), 3.48 (ddd, J = 11.0, 9.5, 2.4 Hz, 1H), 3.40 (ddd, J = 11.0, 8.5, 3.4 Hz, 1H), 3.37 (m, 2H), 3.25(ddd, J = 15.5, 6.0, 2.7 1H), 3.15 (m, 2H), 3.00 (ddd, J = 15.0, 11.5, 6.0, 1H), 2.95 (ddd, J = 10.0, 4.8, 4.0 Hz, 1H), 2.76 (m, 2H), 2.60 (ddd, J = 13.0, 7.5, 2.4 Hz, 1H), 2.46 (dd, J = 12.0, 6.5 Hz, 1H) ; ^{13}C NMR (125.6 MHz, CD_3OD) δ 214.7, 211.6, 147.3, 139.4, 137.8, 137.1, 135.8, 133.5, 130.7, 129.6, 129.3, 128.7 128.4, 127.5, 127.3, 126.0, 124.4, 102.5, 85.5, 77.5, 76.4 70.9, 64.4, 61.3, 57.6, 51.2, 50.2, 41.0, 32.6, 29.2; HRMS: calculated for C_{31} H_{31} N O_7 Na 552.1998; found 552.1996

Supplemental Material

Characterization data for **3**, **12**, **13** including COSY and CD analysis, X-Ray coordinates for **10**, and oligonucleotide preparation procedures and binding methods are available as supplemental material. Please write to chembiol@cell.com for a PDF.

Acknowledgments

Research in the Goldberg and Jones laboratories was supported by the National Institute of General Medical Sciences.

Received: May 17, 2002
Revised: June 28, 2002
Accepted: July 1, 2002

References

1. Sanger, W. (1994). Principles of Nucleic Acid Structure. (New York: Springer-Verlag).
2. Turner, D.H. (1992). Bulges in nucleic acids. Curr. Opin. Struct. Biol. *2*, 334–337.
3. Chastain, M., and Tinoco, I. (1991). Structural elements in RNA. In Progress in Nucleic Acid Research and Molecular Biology, W.E. Cohn, K. Moldave. eds. (New York: Academic) *41*, 131–177.
4. Lilley, D.M.S. (1995). Kinking of DNA and RNA by base bulges. Proc. Natl. Acad. Sci. USA *92*, 7140–7142.
5. Dingwall, C., Ernberg, I., Gait, M.J., Green, S.M., Heaphy, S., Karn, J., Lowe, A.D., Singh, M., Skinner, M.A., and Valerio, R. (1989). HIV-1 tat protein binds trans-activation-responsive region (TAR) RNA in vitro. Proc. Natl. Acad. Sci. USA *86*, 6925–6929.
6. Greenblatt, J., Nodwell, J.R., and Mason, S.W. (1993). Transcriptional antitermination. Nature *364*, 401–406.
7. Wells, R.D. (1996). Molecular bases of genetic instability of triplet repeats. J. Biol. Chem. *271*, 2875–2878.
8. Perutz, M.F. (1996). Glutamine repeats and inherited neurodegnerative disease: molecular aspects. Curr. Opin. Struct. Biol. *6*, 848–858.
9. Kunkel, T.A. (1993). Slipping DNA and diseases. Nature *365*, 207–209.
10. Harvey, S.C. (1997). Slipped structures in DNA triplet repeat sequences: entropic contributions to genetic instabilities. Biochemistry *36*, 3047–3049.
11. Xi, Z., and Goldberg, I.H. (1999). DNA-damaging enediyne compounds. In Comprehensive Natural Products Chemistry, D.H.R. Barton and K. Nakanishi, eds. (Oxford: Pergamon) *7*, 553–592.
12. Xi, Z., Mao, Q.-K., and Goldberg, I.H. (1999). Mechanistic studies on the base catalyzed transformation of neocarzinostatin chromophore: Roles of bulged DNA. Biochemistry *38*, 4342–4354.
13. Kappen, L.S., and Goldberg, I.H. (1993). DNA conformation-induced activation of an enediyne for site-specific cleavage. Science *261*, 1319–1321.
14. Kappen, L.S., and Goldberg, I.H. (1993). Site-specific cleavage at a DNA bulge by neocarzinostatin chromophore via a novel mechanism. Biochemistry *32*, 13138–13145.
15. Kappen, L.S., and Goldberg, I.H. (1995). Bulge-specific cleavage in transactivation response region RNA and its DNA analogue by neocarzinostatin chromophore. Biochemistry *34*, 5997–6002.
16. Hensens, O.D., Chin, D.-H., Stassinopoulos, A., Zink, D.L., Kappen, L.S., and Goldberg, I.H. (1994). Spontaneous generation of a biradical species of neocarzinostatin chromophore: Role in DNA bulge-specific cleavage. Proc. Natl. Acad. Sci. USA *91*, 4534–4538.
17. Yang, C.F., Stassinopoulos, A., and Goldberg, I.H. (1995). Specific binding of the biradical analog of neocarzinostatin chromophore to bulged DNA: Implications for thiol-independent cleavage. Biochemistry *34*, 2267–2275.
18. Stassinopoulos, A., Ji, J., Gao, S., and Goldberg, I.H. (1996). Solution structure of a two-base DNA bulge complexed with an enediyne cleaving analog. Science *272*, 1943–1946.
19. Gao, X., Stassinopoulos, A., Ji, J., Kwon, Y., Bare, S., and Goldberg, I.H. (2002). Induced formation of a DNA bulge structure by a molecular wedge ligand-postactivated neocarzinostatin chromophore. Biochemistry *41*, 5131–5143.
20. Myers, A.G., Liang, J., Hammond, M., Harrington, P., Wu, Y., and Kuo, E. (1998). Total synthesis of the (+)-neocarzinostatin chromophore. J. Am. Chem. Soc. *120*, 5319–5320.
21. Smith, A.L., and Nicolaou, K.C. (1996). The enediyne antibiotics. J. Med. Chem. *39*, 2103–2117.
22. Grissom, J.W., Gunawardena, G.U., Klingberg, D., and Huang, D. (1996). The chemistry of enediynes, enyne allenes and related compounds. Tetrahedron *52*, 6453–6518.
23. Maier, M.E. (1995). Design of Enediyne Prodrugs. Synlett, 13–26.
24. Xi, Z., Jones, G.B., Qabaja, G., Wright, J.W., Johnson, F.S., and Goldberg, I.H. (1999). Synthesis and DNA binding of spirocyclic model compounds related to the neocarzinostatin chromophore. Org. Lett. *1*, 1375–1377.
25. Butkus, E., Berg, U., Stoncius, A., and Rimkus, A. (1998). Chromatographic enantiomer separation and absolute configuration of spiro[benzo-1,3-dioxole-2,9'-bicyclo[3.3.1]nonan]-2'-one and the corresponding diastereomeric hydroxy acetals. J. Chem. Soc. Perkin Trans. *2*, 2547–2551.
26. Morris, J.L., Becker, C.L., Fronczek, F.R., Daly, W.H., and McLaughlin, M.L. (1994). Synthesis of extended linear aromatics using tandem Diels-Alder aromatization reactions. J. Org. Chem. *59*, 6484–6486.
27. Minuti, L., Taticchi, A., Gacs-Baitz, E., and Marrocchi, A. (1995). High pressure Diels-Alder reactions of 2-vinyl-3,4-dihydronaphthalene. Synthesis of cyclopenta[c]- and Indeno[c]phenanthrenones. Tetrahedron *51*, 8953–8958.